

# Structural and Physical Properties of $\tau$ -(EDO-*S,S*-DMEDT-TTF)<sub>2</sub>(AuBr<sub>2</sub>)<sub>1+y</sub> and $\tau$ -(P-*S,S*-DMEDT-TTF)<sub>2</sub>(AuBr<sub>2</sub>)<sub>1+y</sub>

G. C. Papavassiliou, G. A. Mousdis, G. C. Anyfantis, K. Murata<sup>a</sup>, L. Li<sup>a</sup>, H. Yoshino<sup>a</sup>, H. Tajima<sup>b</sup>, T. Konoike<sup>c</sup>, J. S. Brooks<sup>d</sup>, D. Graf<sup>d</sup>, and E. S. Choi<sup>d</sup>

Theoretical and Physical Chemistry Institute, NHRF,  
48 Vassileos Constantinou Ave., Athens 116-35, Greece

<sup>a</sup> Graduate School of Science, Osaka City University, Sumiyoshi-ku, Osaka 558-8585, Japan

<sup>b</sup> Institute for Solid State Physics, University of Tokyo,  
Kashiwanoha, Kashiwa-shi, Chiba 277-8581, Japan

<sup>c</sup> National Institute for Material Science, 3-13 Sakura, Tsukuba, Ibaragi 305-0003, Japan

<sup>d</sup> National High Magnetic Field Laboratory and Physics Department, Florida State University,  
Tallahassee, Florida 32310, USA

Reprint requests to Prof. G. C. P.; Fax: 30210-7273794, E-mail: pseria@eie.gr

Z. Naturforsch. **59a**, 952–956 (2004); received March 31, 2004

Some new findings concerning the structural, optical, transport and magnetotransport properties of  $\tau$ -(EDO-*S,S*-DMEDT-TTF)<sub>2</sub>(AuBr<sub>2</sub>)<sub>1+y</sub> and  $\tau$ -(P-*S,S*-DMEDT-TTF)<sub>2</sub>(AuBr<sub>2</sub>)<sub>1+y</sub> ( $y \approx 0.75$ ) are reported. Some similarities and dissimilarities in the properties are discussed. The dissimilarities are more pronounced at low temperatures and high magnetic fields. The results are compared to those obtained of other conducting multilayered systems.

**Key words:** Organic Conductors; Crystal Structure; Electronic Structure; Optical Properties; Conductivity; Magnetotransport.

## 1. Introduction

Organic-inorganic hybrid conductors of the  $\tau$ -phase are composed of organic cation radical and ordered-linear-anion layers that are separated from each other by disordered-linear-anion layers, forming a unit cell of the tetragonal system (see [1–8] and refs. therein). Only a small number of unsymmetric  $\pi$ -donor molecules gave cation radical salts of the  $\tau$ -phase [1]. Most work has been done on  $\tau$ -(EDO-*S,S*-DMEDT-TTF)<sub>2</sub>(AuBr<sub>2</sub>)<sub>1+y</sub> (EDO) and  $\tau$ -(P-*S,S*-DMEDT-TTF)<sub>2</sub>(AuBr<sub>2</sub>)<sub>1+y</sub> (PT) ( $y \approx 0.75$ ).

In this paper, some new findings concerning the structural, optical, transport and magnetotransport properties of the quasi-2-dimensional compounds EDO and PT are reported. Some similarities and dissimilarities in the properties of these compounds are discussed. The results are compared to those obtained of other conducting multilayered systems [9–19].

## 2. Experimental

Crystals of the corresponding donor molecules were obtained by methods reported in [1, 2, 5, 6]. The in-

strumentation reported in [3–7] was used for the measurements. The resistance and magnetoresistance were measured by the dc four-terminal method. The Hall resistance was measured by a four- or six-terminal method.

## 3. Results and Discussion

### 3.1. Structural Properties

The compounds of the  $\tau$ -phase crystallized in the form of platelets showing several habits (tabular, pyramidal, prismatic, lamellar, bipyramidal etc.). In all cases, the larger surface of the crystals is parallel to the (highly conducting) *ab*-plane, i. e., perpendicular to the *c*-axis.

Electronic band structure calculations based on the X-ray crystallographic data of EDO and PT at room temperature gave a star-like Fermi surface, with a 12.5% area of the first Brillouin zone for  $y = 0.75$ , as is shown in Fig. 1a (see [5–7] and refs. therein). Diffuse X-ray scattering patterns, obtained from measurements at room temperature as well as at lower temperatures (ca. 14 K), showed that in these salts the conducting (: organic) layer and the insulating anion layer form

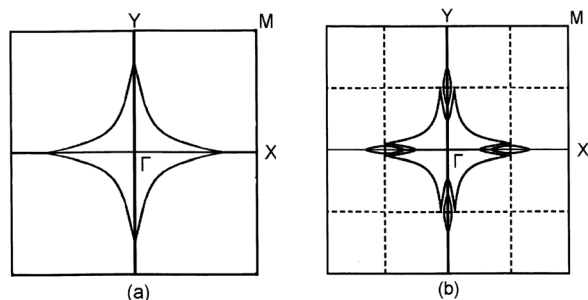


Fig. 1. Calculated Fermi surface of EDO. (a) Using X-ray crystallographic data for  $y = 0.75$ . (b) Reconstructed Fermi surface, taking into account the superstructure data for  $y = 0.875$ .

independent lattices. In EDO, superstructure has been observed below ca. 230 K [4, 5]. It consists of clear satellite reflections between the centers of the Bragg spots. These results led to a reconstruction of half of the Fermi surface. At  $y = 0.875$ , a Fermi surface with two pockets was found, i. e., 1.2% and 6.1% of the first Brillouin zone, as is shown in Fig. 1b [4, 5]. The reconstruction of the Fermi surface has been described for similar multilayered systems (see [13, 19] and refs. therein). In PT no superstructure was observed even at 14 K.

### 3.2. Optical Properties

Figure 2 shows room temperature polarized reflectance spectra obtained from a single crystal of EDO with a tabular shape. The spectrum obtained from the normal incidence on the large surface (ab-plane) with the electric vector of the light parallel to the  $a$ - or  $b$ -axis ( $E//a,b$ ) is identical with that reported previously [8]. It is related with the intermolecular interactions through the heteroatoms of several species of the donor molecules in the ab-plane, and the corresponding transfer integrals. Additionally, the polarized spectrum observed from a lateral surface with the electric vector of light parallel to the  $c$ -axis ( $E//c$ ) is reported therein. It is related to the intramolecular excitations of several species of the donor molecules oriented parallel to the  $c$ -axis. One can see that there is a large anisotropy between the two directions. The reflectivity data for  $E//a,b$  are fitted well with a Drude-Lorentz model. The spectrum with  $E//a,b$  shows a band at ca.  $5500\text{ cm}^{-1}$ , which is attributed to charge-transfer excitation between the species (EDO- $S,S$ -DMEDT-TTF) $^{+\bullet}$ , driven by the onsite Coulomb repulsion (see [5, 8] and refs. therein). Due to this band,

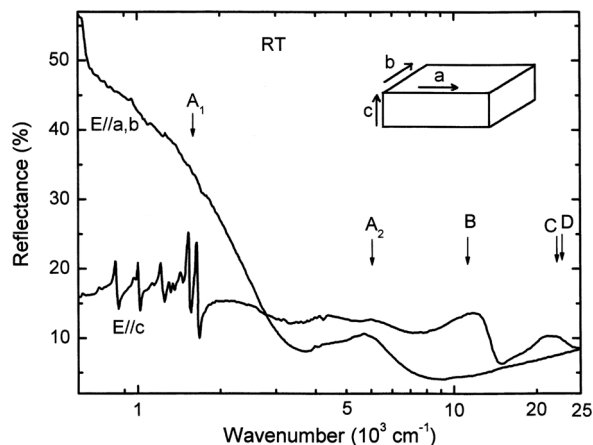


Fig. 2. Room temperature polarized reflectance spectra from a single crystal of EDO with a tabular shape. The arrows  $A_1$ ,  $A_2$ , B, C and D indicate the position of the corresponding bands in the OA spectrum of material dispersed in a KBr pellet.

the Drude edge is not clear in the  $E//a,b$  spectrum. The spectrum with  $E//c$  shows a strong vibrational feature in the infrared spectral region. Kramers-Kronig analysis of the reflectance data with  $E//c$  gave the optical conductivity spectrum with strong peaks at  $1446$  and  $1535\text{ cm}^{-1}$ . The corresponding OA spectrum of the neutral donor molecules showed a weak peak at  $1447$ , a very weak one at ca.  $1530$  and a medium one at  $1651\text{ cm}^{-1}$  [1, 8]. The OA spectra of EDO dispersed in a KBr pellet or rubbed on a quartz plate, showed both, the parallel and perpendicular spectra. The electronic OA bands are indicated by the arrows  $A_1$ ,  $A_2$ , B, C and D in Figure 2. Identical spectra were observed from crystals with several other habits. The polarized reflectance spectra of PT crystals of several habits with  $E//a,b$  showed reflectivity values of 35–42% at ca.  $600\text{ cm}^{-1}$  (see also [2, 5]). In all crystals examined the reflectivities are smaller than the corresponding values of EDO, especially at low frequencies. This indicates that the metallic behavior of EDO is better than that of PT. The spectrum with  $E//a,b$  shows the same band at ca.  $5500\text{ cm}^{-1}$  as that of EDO. The spectrum obtained from a lateral surface showed the vibrational features in the infrared spectral region with a strong band at ca.  $1375\text{ cm}^{-1}$ . The OA spectrum of material dispersed in a KBr pellet or rubbed on a quartz plate showed the features of both polarizations, with electronic bands and vibrational bands [1, 2]. In both cases, the OA spectra showed a common band at ca.  $5500\text{ cm}^{-1}$ . The vibrational bands around  $1400\text{ cm}^{-1}$

are characteristic of C=C central bonds and, in addition to UV-visible spectra, allow the composition identification of several species (see [1]).

### 3.3. Transport Properties

The in-plane resistivity ( $\rho_{ab}$ ) of PT shows a metallic temperature dependence down to low temperatures with an upturn at ca. 10 K and a weak crossover at ca. 120 K. The out-of-plane resistivity ( $\rho_c$ ) shows semiconducting behavior down to low temperatures, a crossover at ca. 20 K and an upturn of the resistivity at ca. 5 K, see [5, 7]. The metal to semiconductor (or insulator) transition at low temperatures may be due to weak localization effects [11, 12]. The resistivity anisotropy  $\rho_c/\rho_{ab}$  is of the order  $10^3$  at room temperature and much higher at low temperatures. The in-plane resistivity of EDO shows a metallic temperature dependence with an upturn at 30–50 K. The out-of-plane resistivity varies from crystal to crystal (see [4–6] and refs. therein). Some crystals exhibit an upturn of the

resistivity at ca. 30–40 K (see for example the inset of Figure 3a). Some other crystals exhibit weak metallic behavior down to very low temperatures (ca. 0.4 K) (see for example the inset of Figure 3b). The resistivity anisotropy is of the order  $10^3$ – $10^4$ .  $\rho_c$  decreased on applying pressure [5]. It should be noted that the temperature dependence of the resistivity and the resistivity anisotropy of the  $\tau$ -phase conductors reported above are similar to those observed in other layered metallic systems, such as  $\text{Sr}_2\text{RuO}_4$ ,  $(\text{Bi,Pb})_2\text{Sr}_3\text{Co}_2\text{O}_9$ , and  $(\text{TMTSF})_2\text{PF}_6$  (see [10–12] and refs. therein).

### 3.4. Magnetotransport Properties

At low fields the magnetoresistance behavior varies from crystal to crystal. Semiconducting crystals exhibit negative magnetoresistance, while metallic crystals exhibit positive magnetoresistance. The magnetic field dependence of the out-of-plane magnetoresistance of a semiconducting crystal is shown in Fig. 3a, and that of a metallic crystal in Fig. 3b of EDO at 0.45 K. The temperature dependences of  $R_c$  at  $B=0$  are shown in the corresponding insets of Figure 3. One can see that the semiconducting crystal exhibits negative magnetoresistance, especially at low fields, while the metallic crystal exhibits positive magnetoresistance. At moderate and higher fields both crystals exhibit slow Shubnikov-de Haas (SdH) oscillations of frequency 47.2 and 43.8 T, and fast oscillations of 460 and 471 T, respectively. These frequencies correspond to ca. 0.66% and 6.1% of the first Brillouin zone, respectively. They are close to those obtained from a reconstructed Fermi surface (Fig. 1b). The behavior is similar to that observed in  $(\text{TMTSF})_2\text{ClO}_4$  [19]. Crystals of PT exhibit negative magnetoresistance at low fields and fast SdH oscillations at higher fields (see also [3–7]), with frequencies close to those of EDO, as well as weak slow oscillations of ca. 180 T [6, 7]. The compound exhibits an upturn of the magnetoresistance near ca. 35 T [3]. Considerable differences were found in the magnetoresistance behavior of EDO and PT at high pressure. The results will be published separately.

In a crystal of EDO (#0212) with a semiconducting behavior, like that of the crystal #0211 (inset of Fig. 3a), the magnetic field dependence of the in-plane resistance ( $R_{xx}$ ) and Hall resistance ( $R_{xy}$ ) were measured by making contacts on the surface (ab-plane) of the crystal. The results obtained at 0.6 K are shown in Figure 4. One can see that at low fields  $R_{xx}$  de-

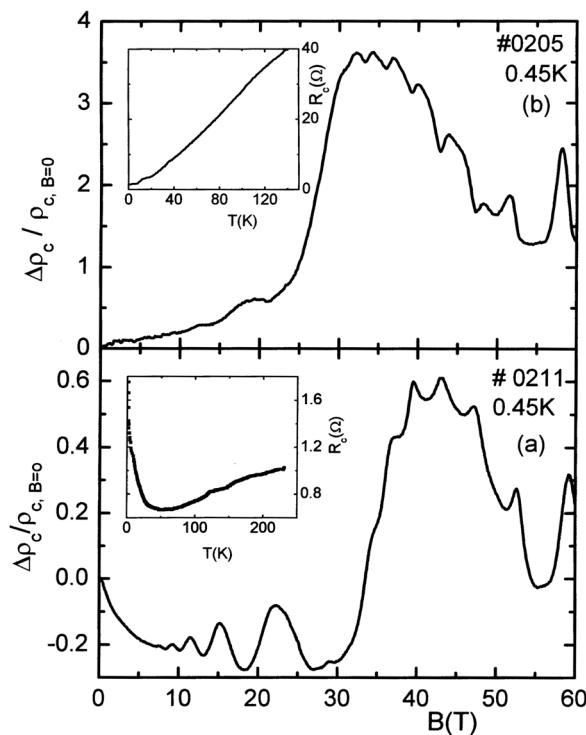


Fig. 3. (a) Magnetic field dependence of the out-of-plane magnetoresistance of a semiconducting crystal, (b) a metallic crystal of EDO at 0.45 K. The insets show the corresponding temperature dependence of the out-of-plane resistance ( $R_c$ ) at  $B=0$ .

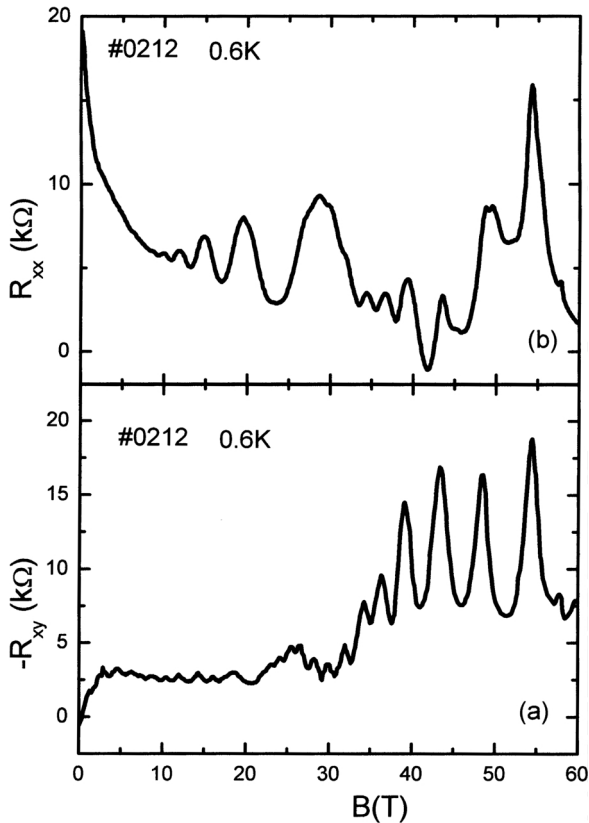


Fig. 4. Measured field dependencies of  $R_{xx}$  and  $R_{xy}$  in a crystal of EDO at 0.6 K, by making contacts on the surface (ab-plane) of the crystal.

creases with increasing the magnetic field, and at higher fields SdH oscillations are observed, as in the out-of-plane resistance  $R_{zz}$  (Fig. 3a).  $R_{xy}$  is not proportional to the strength of the magnetic field but exhibits flat structures (plateaus) that reminds the quantum Hall (QH) effect, observed in a number of semiconductor multilayered systems, such as semiconductor superlattices [9, 14–18]. In these systems, when the Fermi energy falls between extended state bands, a QH state is expected, with vanishing bulk diagonal conductivities ( $\sigma_{xx}$ ), and quantized  $\sigma_{xy} = -ije^2/h$ , where  $i(= 1, 2, 3 \dots)$  is the Landau level index and  $j$  the number of layers connected in parallel [9, 16–18]. The corresponding Hall resistance could be written as

$$R_{xy} = -h/ije^2. \quad (1)$$

For  $i = 1$  and  $j = 1$ ,  $R_{xy} = -25.813 \text{ k}\Omega$ .

This is the resistance of one layer. If we compare Figs. 4a, 4b and 3a, we can see that the Hall plateau

( $i = 1$ , in Fig. 4a) coincides perfectly with the minimum in  $R_{xx}$  (Fig. 4b) and the maximum in  $R_{zz}$  (Fig. 3a) around 45 T, where the quantum limit occurs, as it is described in similar systems [9, 14–19]. However, the best coincidence of the experimental data (of Fig. 4a) with (1) is obtained if we consider that the penetration depth of the contacts is not  $j = 1$ , but  $j = 4$  (layers). Then, from (1) with  $i = 1$  and  $j = 4$  one finds  $R_{xy}(1, 4) = -6.45 \text{ k}\Omega$ , which is close to that obtained from the first plateau of Fig. 4a, i.e., ca.  $-7 \text{ k}\Omega$ . Also, from (1) with  $i = 2$  and  $j = 4$  one finds  $R_{xy}(2, 4) = -3.22 \text{ k}\Omega$ , which is close to the value of the second plateau of Fig. 4a, i.e., ca.  $-2.7 \text{ k}\Omega$ . Some discrepancies between experiment and theory observed for  $R_{xy}$ , are similar to those observed in a number of other multilayered systems [9, 14–19]. They could be attributed to interlayer interactions, tunneling, and other effects, as in [5, 10]. In the crystals of PT,  $R_{xy}$  is almost proportional to the magnetic field and does not show any QH plateau at high fields, while the  $R_{xx}$  behavior is similar to that of  $R_{zz}$  [3, 7].

In another crystal of EDO (#B2003) with semiconducting behavior, like that of #0211 (Fig. 3a), the out-of-plane magnetoresistance  $R_{zz}$  was measured for 17 temperatures, from 14 to 0.52 K. Figure 5 shows the temperature dependence of  $R_{zz}$  at ca. 44 T ( $i = 1$ ) and ca. 24 T ( $i = 2$ ). The magnetic field dependence of  $R_{zz}$  at 14.0, 3.0 and 0.52 K is shown in the inset of Figure 5. One can see that above 4 K,  $R_{zz}$  shows an Arrhenius-type temperature dependence, indicating that the dominant vertical transport is through the bulk

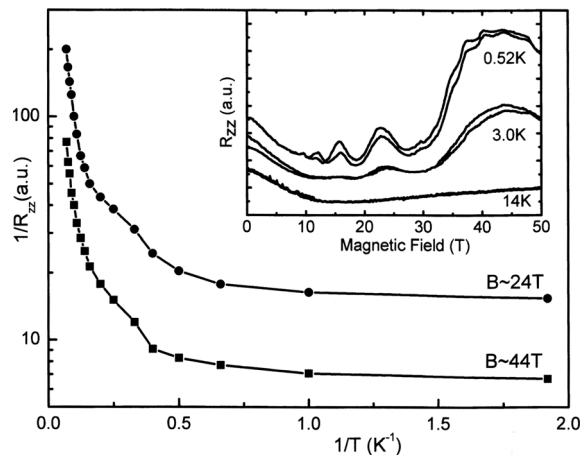


Fig. 5. Temperature dependence of the out-of-plane magnetoresistance  $R_{zz}$  at ca. 44 T and ca. 24 T from a crystal of EDO ( $\neq$ B2003). The inset shows the magnetic field dependence of  $R_{zz}$  at 14.0, 3.0 and 0.52 K.

states at high temperatures. Below 2 K,  $R_{zz}$  tends to saturate, indicating that the transport (created by tunneling) is over the surface (: chiral surface states). In another crystal (#0315) with semiconducting behavior the temperature dependence of  $R_{zz}$  (at ca. 44 T) is close to that of #B2003 in the temperature range from 4.3 to 0.47 K. Also, preliminary measurements of the in-plane magnetoresistance  $R_{xx}$  at different temperatures showed that the  $R_{xx}$ -minima remain finite in the low temperature limit ( $\leq 2$  K). However, as in the case of the QH systems  $(\text{TMTSF})_2\text{ClO}_4$  [19] and  $\eta\text{-Mo}_4\text{O}_{11}$  as well as in some systems based on GaAs-AlGaAs [9, 14–18],  $R_{zz}$  is not flat in the QH states ( $i = 1, 2, \dots$ ). In a crystal of EDO (#0205) with metallic behavior (see Fig. 3b), the Arrhenius-type temperature dependence of  $R_{zz}$  at ca. 31 T occurs above 0.5 K. More experiments for the confirmation of the chiral surface states in  $\tau$ -phase conductors are planned.

#### 4. Conclusions

The structural, optical, transport and magnetotransport properties in the  $\tau$ -phase conductors EDO and PT show slight differences from crystal to crystal of the same compound, but considerable differences from compound to compound, especially at low temperatures and high magnetic fields. The properties were found to be similar to those obtained in other systems with multilayered structures. The  $\tau$ -phase conductors seem to be similar to modulation doped semiconductors (e.g., compounds based on GaAs/AlGaAs) [14–16, 19] rather than similar to Mott doped insulators (e.g., compounds based on  $\text{CuO}_2$ ) [10, 13]. The compound EDO exhibits semiconducting behavior at very low temperatures and slow SdH oscillations, which are related to the QH states. This is an interesting system for further investigation.

- [1] G. C. Papavassiliou, in: J. Yamada and T. Sugimoto (Eds.), TTF Chemistry, Kodansha and Springer, Tokyo 2004, Chapt. 2.
- [2] A. Lapinski, A. Graja, G. C. Papavassiliou, and G. A. Mousdis, *Synth. Met.* **139**, 405 (2003).
- [3] J. S. Brooks, D. Graf, E. S. Choi, L. Balicas, K. Storr, C. H. Mielke, and G. C. Papavassiliou, *Phys. Rev. B* **67**, 153104 (2003).
- [4] T. Konoike, K. Iwashita, I. Nakano, H. Yoshino, T. Sasaki, T. Takahashi, Y. Nogami, J. S. Brooks, D. Graf, C. H. Mielke, G. C. Papavassiliou, and K. Murata, *Synth. Met.* **135–136**, 615 (2003).
- [5] T. Konoike, PhD Thesis, Osaka State Univ. (2003).
- [6] T. Konoike, K. Iwashita, H. Yoshino, K. Murata, T. Sasaki, and G. C. Papavassiliou, *Phys. Rev. B* **66**, 245308 (2002).
- [7] K. Storr, L. Balicas, J. S. Brooks, D. Graf, and G. C. Papavassiliou, *Phys. Rev. B* **64**, 45107 (2001).
- [8] I. Olejniczak, J. L. Musfeldt, G. C. Papavassiliou, and G. A. Mousdis, *Phys. Rev. B* **62**, 15634 (2000).
- [9] H. Aoki, *Physica E* **20**, 149 (2003).
- [10] T. Valla, P. D. Johnson, Z. Yusof, B. Wells, Q. Li, S. M. Loureiro, R. J. Cava, M. Mikami, Y. Mori, M. Yoshimura, and T. Sasaki, *Nature London* **417**, 627 (2002); I. Tsukada, T. Yamamoto, M. Takaki, T. Tsubone, S. Konno, and K. Uchinokura, *J. Phys. Soc. Japan* **70**, 834 (2001); M. Kuraguchi, E. Ohmichi, T. Osada, and Y. Shiraki, *Synth. Met.* **133–134**, 113 (2003).
- [11] Y. H. Yang, *Physica B* **305**, 143 (2001).
- [12] M. Suzuki, I. S. Suzuki, K. Matsubara, and K. Sugi-hara, *Phys. Rev. B* **61**, 5013 (2000).
- [13] E. G. Maksimov, *Phys. Usp.* **43**, 965 (2000); S. G. Ovshinnikov, *Phys. Usp.* **46**, 21 (2003); R. Tamazyan, S. vanSmaalen, I. Grigorevna Vasilyeva, and H. Arnold, *Acta Cryst.* **B59**, 709 (2003).
- [14] B. Zhang, J. Brooks, Z. Wang, J. Simmons, J. Reno, N. Lumpkin, J. O'Brien, and R. Clark, *Phys. Rev. B* **60**, 8743 (1999).
- [15] M. Kawamura, A. Endo, S. Katsumoto, Y. Iye, C. Terakura, and S. Uji, *Physica B* **298**, 48 (2001).
- [16] D. P. Druist, P. J. Turley, K. D. Maranowski, E. G. Gwinn, and A. C. Gossard, *Phys. Rev. Lett.* **80**, 365 (1998).
- [17] S. Hill, J. S. Brooks, S. Uji, M. Takashita, C. Tarashima, H. Aoki, Z. Fisk, and J. Sarrao, *Synth. Met.* **103**, 2667 (1999).
- [18] H. L. Störmer, J. P. Eisenstein, A. C. Gossard, W. Wiegmann, and K. Baldwin, *Phys. Rev. Lett.* **56**, 85 (1986); H. L. Störmer, J. P. Eisenstein, A. C. Gossard, K. W. Baldwin, and J. H. English in: O. Engstrom (Ed.) *Proc. 18<sup>th</sup> Int. Conf. Phys. Semiconductors*, World Scientific p. 385, (1987).
- [19] N. Matsunaga, A. Ayari, P. Monceau, A. Ishikawa, K. Nomura, M. Watanabe, J. Yamada, and S. Nakatsuji, *Phys. Rev. B* **66**, 24425 (2002); S. Uji, C. Terakura, T. Terashima, J. S. Brooks, S. Tanaka, S. Maki, S. Nakatsuji, and J. Yamada, *Synth. Met.* **120**, 975 (2001).